




A comparative study of melanocytic nevi classification with dermoscopy and high-frequency ultrasound

Yu-Kun Wang^{1,#}  | Yuan-Jing Gao^{2,#} | Jie Liu¹ | Qing-Li Zhu²  |
Jun-cheng Wang¹  | Jing Qin² | Hong-Zhong Jin¹

¹ Department of Dermatology, Peking Union Medical College Hospital, Center for Translational Medicine, Chinese Academy of Medical Sciences and Peking Union Medical College, Beijing, China

² Department of Ultrasound, Peking Union Medical College Hospital, Chinese Academy of Medical Sciences and Peking Union Medical College, Center for Translational Medicine, Beijing, China

Correspondence

Jie Liu, Department of Dermatology, Peking Union Medical College Hospital, Chinese Academy of Medical Sciences and Peking Union Medical College, Center for Translational Medicine, Beijing 100730, China.
Email: Liujie04672@pumch.cn

Qing-Li Zhu, Department of Ultrasound, Peking Union Medical College Hospital, Chinese Academy of Medical Sciences and Peking Union Medical College, Center for Translational Medicine, Beijing 100730, China.
Email: zqlpumch@126.com

#Yu-Kun Wang and Yuan-Jing Gao contributed equally to this article.

Funding information

The Non-profit Central Research Institute Fund of Chinese Academy of Medical Sciences, Grant/Award Number: 2019XK320024; National Natural Science Foundation of China, Grant/Award Number: 61871011; The CAMS Innovation Fund for Medical Sciences (CIFMS), Grant/Award Number: 2020-I2M-C&T-B-033

Abstract

Background: Melanocytic nevi (MN) can be classified into three subtypes according to the depth of the nests of nevus cells which is important for management. High-frequency ultrasound (HF-US) can clearly reveal the lesion size, contour, depth, and internal structures. However, the HF-US studies of MN according to subtypes are limited. We aimed to describe the HF-US features of MN and explore its value in accurate classification.

Materials and methods: This retrospective study was conducted from January 2018 to November 2019. Eighty-five patients with MN were included and examined by 50 and 20 MHz HF-US. The HF-US features were recorded including morphological flatness, depth, shape, boundary, internal echogenicity, hyperechoic spots, lateral acoustic shadow, posterior echoic patterns, mushroom signs, and straw-hat signs. Each image was evaluated by two physicians independently, and the consistency was tested.

Results: Eleven lesions could not be detected by HF-US. The rest 74 lesions underwent ultrasonic analysis. MN appeared as strip-shaped or oval, hypoechoic areas localized in the epidermis and dermis under ultrasonography. A strong consistency between HF-US and dermoscopy of determining the lesion depth was achieved ($\kappa = 0.935$, $p < 0.001$). The hyperechoic spots were found in 57.6% intradermal nevi. The mushroom signs were seen in 34.8% intradermal nevi, and the straw-hat signs were seen in all the compound nevi.

Conclusion: MN can be correctly classified using HF-US, and it had a strong correlation with dermoscopic and clinical classification. HF-US could further reveal the internal morphological features of MN, which may support more precise classification and management.

KEYWORDS

dermoscopy, high-frequency ultrasound, melanocytic nevus, mole, skin imaging

Abbreviations: HF-US, high-frequency ultrasound; MN, melanocytic nevus (nevi)

This is an open access article under the terms of the [Creative Commons Attribution-NonCommercial-NoDerivs](https://creativecommons.org/licenses/by-nc-nd/4.0/) License, which permits use and distribution in any medium, provided the original work is properly cited, the use is non-commercial and no modifications or adaptations are made.

© 2021 The Authors. *Skin Research and Technology* published by John Wiley & Sons Ltd.

1 | INTRODUCTION

Melanocytic nevi (MN), usually referred to common acquired MN or moles, are benign proliferations of nevus cells and among the most frequently encountered neoplasms in dermatology clinics.¹⁻⁴ Histologically, according to the depth of the nests of nevus cells, MN can be divided into three subtypes, namely junctional nevi (of which the nevus cells locate merely at the dermal-epidermal junction), compound nevi (of which the nests appear both at the dermal-epidermal junction and in the dermis), and intradermal nevi (where the nests of nevus cells are situated in the dermis only). The precise classification is of great value for differential diagnosis and management.

Dermoscopy is the most widely used tool which has already shown its remarkable value in differentiating MN from melanoma and other cutaneous malignancies.^{5,6} Currently, the diagnosis of MN subtypes is also mainly based on clinical and dermoscopic manifestations. However, clinical and dermoscopic features of MN lesions provided mainly horizontal information, thus to indirectly infer the infiltration depth (or the subtype classification).⁷ Moreover, for such a benign tumor, a simultaneous biopsy for imaging-pathological comparison study is not always accessible because of ethical considerations. As a result, the accuracy of clinical and dermoscopic MN classification is unclear. Therefore, further comparative study on the MN classification will help to the diagnosis and management.

High-frequency ultrasound (HF-US) using transducers >20 MHz is capable to reveal the vertical cutaneous structures clearly. With the valuable information of lesion size, contour, depth, and internal structures provided by HF-US, the non-invasive diagnosis of various benign or malignant cutaneous neoplasms and inflammatory skin diseases has gained traction in clinical practice.⁸ However, the HF-US studies of MN are limited,^{9,10} and none of them compared the clinical and dermoscopic manifestations with the ultrasonic features according to MN subtypes.

Therefore, we conducted this retrospective, observational study to explore the application value of HF-US in the clinical evaluation of MN, summarize the detailed HF-US features of MN classifying to subtypes, and put forward their histologic foundation for the first time.

2 | MATERIALS AND METHODS

2.1 | Study design and patients

In this study, we retrospectively reviewed the baseline clinical information, dermoscopic images as well as HF-US images of patients with MN from the skin image database of the Department of Dermatology, Peking Union Medical College Hospital from January 2018 to November 2019. The inclusion criteria were as follows: (1) Confirmed diagnosis by two senior dermatologists based on the medical history, clinical manifestations, dermoscopic evaluation, and at least 1-year monitoring. Histopathologic results were acquired for atypical cases. (2) No exposure to any treatment such as carbon dioxide laser and surgical removal before the presentations. The exclusion criteria were as fol-

lows: (1) patients with multiple lesions but the clinical, dermoscopic, and HF-US images could not be accurately matched. (2) Patients with other skin disorders nearby the investigated MN lesions. (3) Patients with incomplete clinical information or images.

2.2 | Ethics

This study was approved by the Medical Ethics Committee of Peking Union Medical College Hospital in May 2019 (NO. JS-2003), and all the included patients provided written informed consent.

2.3 | Clinical and dermoscopic evaluation

Patients with MN were initially diagnosed and classified into three subtypes according to following clinical and dermoscopic criteria¹¹:

1. Junctional nevi: The lesions were brown to black macules, flat or slightly elevated, and typically manifested as regular pigment networks under dermoscopy.
2. Intradermal nevi: The lesions were mostly skin-colored to black, dome-shaped papules which could be accompanied with terminal hairs and keratotic materials. Dermoscopy of intradermal nevi usually revealed as oval structures consisting of regular globules or clods with terminal hairs and comma-shaped vessels.
3. Compound nevi: The lesions were maculopapules with different extents of pigmentations, and shared dermoscopic features of both junctional nevi and intradermal nevi.

2.4 | examination and image analysis

The HF-US images of the same lesion that previously undergone clinical and dermoscopic assessment were captured by the same operator with both 50 and 20 MHz transducers using an MD-300S type II diagnostic system (Tianjin Media Medical Technology Co., Ltd. China). Afterward, two physicians with experience in dermatologic ultrasound evaluated the HF-US images independently. Agreement was reached through discussion if any discordance occurred. Refer to the previous reports,^{9,10,12} each observer was asked to analyze all the ultrasound images and to describe the following features: morphological flatness (flat, uneven), location of the lesion within the skin layers (epidermis, dermis, or both), shape (oval or strip), boundary (clear or unclear), internal echogenicity (homogeneous or heterogeneous), hyperechoic spots (presence or absence), lateral acoustic shadow (presence or absence), posterior echoic patterns (attenuated or absence), mushroom sign (presence or absence), straw-hat sign (presence or absence). Straw-hat sign consisted of a brim (a strip-like hypoechoic area beneath the epidermis) and a cap (elevated hypoechoic area above the epidermis). Mushroom sign¹⁰ was defined as the combination of an umbrella-shaped hypoechoic area and a stalk-shaped hypoechoic area.

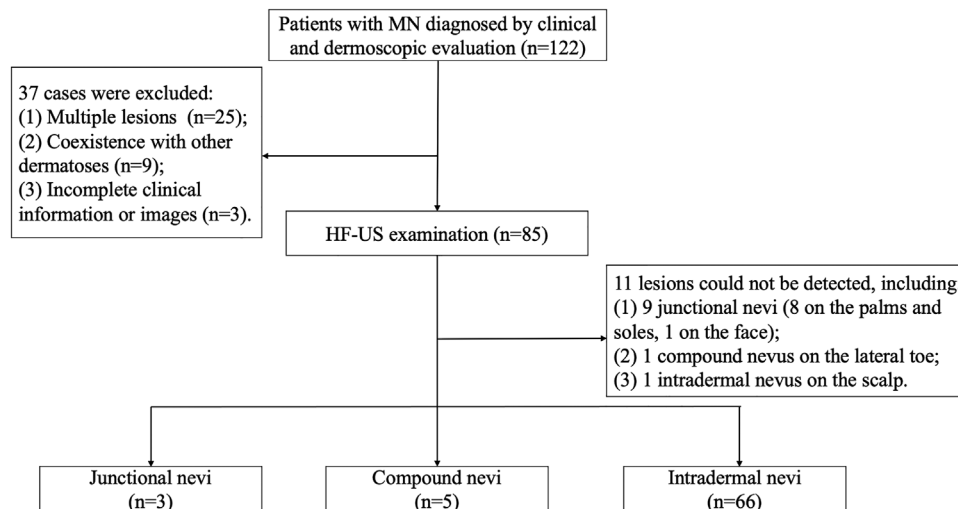


FIGURE 1 Flowchart of this study. HF-US, high-frequency ultrasound; MN, melanocytic nevi

2.5 | Statistical analysis

We used SPSS version 25.0 software (IBM Corporation, Armonk, NY) for statistical analysis. The consistency of assessing ultrasonic features by radiologists was tested by κ test, which was interpreted as follows: $\kappa < 0$, poor agreement; $0 < \kappa < 0.20$, slight agreement; $0.20 < \kappa < 0.40$, fair agreement; $0.40 < \kappa < 0.60$, moderate agreement; $0.60 < \kappa < 0.80$, substantial agreement; and $0.80 < \kappa < 1$, perfect agreement. Significance was set at two-sides $p < 0.05$.

3 | RESULTS

A total of 122 patients with suspected MN were initially included. Thirty-seven patients were excluded for multiple lesions that could not be distinguished apart in our image system ($n = 25$), coexistence with other cutaneous diseases such as nearby folliculitis and solar lentigo lesions ($n = 9$), and incomplete clinical information or images ($n = 3$). Eventually, 85 patients were included for further comparative image analysis. Flowchart of the study was detailed in Figure 1. The baseline information of the patients was listed in Table 1. The mean age of these patients was 34.8 years (range 9–73 years), including 64 women (75.3%) and 21 men (24.7%). The detailed information of dermoscopic features of MN lesions is recorded in Table 2. According to the clinical and dermoscopic evaluation, lesions were classified as 12 junction nevi (14.1%), six compound nevi (7.1%), and 67 intradermal nevi (78.8%).

All of the 85 lesions underwent HF-US examination. However, 11 of them could not be detected by HF-US, including nine (85.7%) junctional nevi (eight cases were on the palms and soles, and one case was on the face), one (16.7%) compound nevus on the lateral toe where it was technically unsteadily to set the probe, and one (1.5%) intradermal nevus on the scalp that covered heavily by hairs. Among the rest 74 cases, the consistency between HF-US and clinical along with dermoscopic evaluation in determining the lesion depth was strong ($\kappa = 0.935$, $p < 0.001$).

TABLE 1 Basic information of the included patients

	Number	Proportion (%)
Total	85	100
Gender		
Male	21	24.7
Female	64	75.3
Subtype		
Intradermal nevus	66	77.6
Compound nevus	6	7.1
Junctional nevus	13	15.3
Location		
Trunk	26	30.6
Face	28	32.9
Head and neck (non-facial area)	8	9.4
Scalp	4	4.7
Acral areas	10	11.8
Arms	2	2.4
Legs	6	7.0
Lip	1	1.2

The ultrasonic features of MN are showed in Table 3. Specifically, all the detected junctional nevi appeared as strip-shaped, homogenous, hypoechoic areas localized in the epidermis and dermal-epidermal junction, without posterior echoic patterns and lateral acoustic shadows (Figure 2). Compound nevi were shown as elevated oval or strip hypoechoic structures infiltrating both epidermis and dermis, and all the compound nevi manifested as straw-hat signs in our cases. We speculate that the dermal nevus cell aggregation at the lesion center appears as the cap, while the continuous band-like nevus cell nests in the dermal-epidermal junction at the lesion periphery contribute the brim to compound nevi (Figure 3). Intradermal nevi presented as

TABLE 2 Most common dermoscopic features of included melanocytic nevus lesions

	Intradermal nevus	Compound nevus	Junctional nevus
Total number	67	6	12
Dermoscopic features			
Hypopigmentation	5	0	0
Pigment network	0	2	3
Pseudo-network	12	1	1
Peripheral reticular with central hypopigmentation	2	0	0
Peripheral reticular with central hyperpigmentation	0	0	2
Homogenous pattern	11	0	0
Peripheral reticular with central globules	3	0	0
Peripheral globules with central network or homogenous area	1	1	0
Globular	37	3	0
Blue-white structures	1	1	0
Parallel furrows pattern	0	1	4
Fibrillar pattern	0	0	2
Lattice-like pattern	0	0	1
Other pigment structures	13	0	0
Milia-like cyst	1	0	0
Comedo-like opening	6	0	0
Shiny white structures	14	1	0
Terminal hair	50	4	1
Comma-like vessels	20	2	0

oval dermal hypoechoic masses, 57.6% cases with internal hyperechoic spots (38/66), 37.9% cases with posterior acoustic attenuations (25/66), and 34.8% cases showing mushroom signs (23/66). The construction of the mushroom sign is associated with the vast number of dermal nevus cells resulting in a dome-shaped or verrucous morphology of the upper part (the umbrella) and the ensheathing of a hair follicle (the stalk) in intradermal nevi (Figure 4).

Notably, straw-hat signs could be found in 100% compound nevi (5/5) and 1.5% intradermal nevus (1/66). Moreover, we found that 34.8% intradermal nevi had mushroom sign (23/66), and this sign appeared almost exclusively in the intradermal nevi, achieving a high specificity of 88.9% to diagnose intradermal nevi. Additionally, hyperechoic spots appeared in 38 intradermal nevus lesions (57.6%), which were speculated to correlate with the melanin accumulations (Figure 5). The inter-operator agreement for the above ultrasonic features ranged from 0.844 to 1.000, indicating a perfect agreement.

4 | DISCUSSION

In this study, we compared the HF-US and dermoscopic evaluation of MN in subtype differentiation for the first time and proved that these two methods had a good consistency, implying that the combination of them could provide accurate and objective information for MN

classification from both vertical and horizontal perspectives. MN have been reported as the most frequently surgically treated neoplasm at the department of dermatology of a tertiary university hospital in China.¹³ Even with the help of dermoscopy, the accurate classification of MN subtypes remains a clinical challenge sometimes depending merely on clinical and dermoscopic criteria. However, to clarify the actual subtypes of MN is meaningful for selecting management strategies, and broadening the understanding of HF-US manifestation of MN could help dermatologists to differentiate it from other diseases such as melanoma. The ultrasonic manifestations of melanoma were reported as homogeneous hypoechoic lesions with clear boundaries and hyperechoic dermis around.¹⁴ In our study, we proposed the ultrasonic characteristics of different types of MN. Through the depth and internal characteristics of the lesions, it is expected to provide more information for the differential diagnosis of melanoma. It is warrant to carry out further study with larger sample size on the HF-US differentiation between melanoma and MN. Besides, although regarded as contraindicated in literature,^{15,16} a lot of patients with cosmetic considerations would come to the hospital and seek for non-surgical treatment of the MN lesions, such as laser ablation, cryotherapy, and electrodesiccation to avoid the postsurgical scar formation. Generally, dermatologists would empirically apply these therapies for once or limited times to MN lesions with small size (usually <6 mm in diameter), flat shape, and no signs of malignancy. But the recurrence and residual

TABLE 3 Ultrasonic features of included and detectable melanocytic nevus lesions

Type	Intradermal nevus	Compound nevus	Junctional nevus	Agreement
N	66	5	3	
Flatness				1.000
Flat	50	4	2	
Uneven	16	1	1	
Boundary				0.964
Clear	51	5	3	
Unclear	14	0	0	
Bulge				0.971
Presence	45	3	0	
Absence	21	2	3	
Depth				0.883
Epidermis	0	0	3	
Epidermis and dermis	1	5	0	
Dermis	65	0	0	
Shape				1.000
Oval	56	2	0	
Strip	10	3	3	
Internal echogenicity				1.000
Homogenous	23	5	3	
Heterogeneous	43	0	0	
Lateral acoustic shadow				0.916
Presence	6	0	0	
Absence	60	5	3	
Posterior acoustic pattern				0.970
Attenuated	25	0	0	
Absence	41	5	3	
Hyperechoic spots				0.973
Presence	38	0	0	
Absence	28	5	3	
Mushroom sign				0.969
Presence	23	1	0	
Absence	43	4	4	
Straw-hat sign				0.844
Presence	1	5	0	
Absence	65	0	3	

Agreement: The κ value of assessing inter-operator agreement of the two readers.

pigmentations are often encountered, perhaps due to inadequate intensity and depth of these destructive methods or mis-judgement for MN subtypes. Junctional nevi with small and flat lesions are more sensitive to treatment, while intradermal and compound nevi with larger and deeper lesions are difficult to remove without recurrence.¹⁶ Our study depicted the detailed HF-US features of MN lesions with different subtypes and might assist the dermatologists to classify MN subtypes, select, and apply treatments more accurately.

Our study demonstrated that combined use of 20 and 50 MHz HF-US could clearly reveal the HF-US characteristic of MN lesions as a well-demarcated hypoechoic structure. There are also other featured manifestations in each MN subtype, expected to corroborate with dermoscopy mutually for the accurate classification. To be specific, junctional nevi were difficult to be detected by HF-US (nine lesions were failed to be revealed in this study). The lesions which were detectable on HF-US appeared as well-defined, strip-shaped hypoechoic areas.

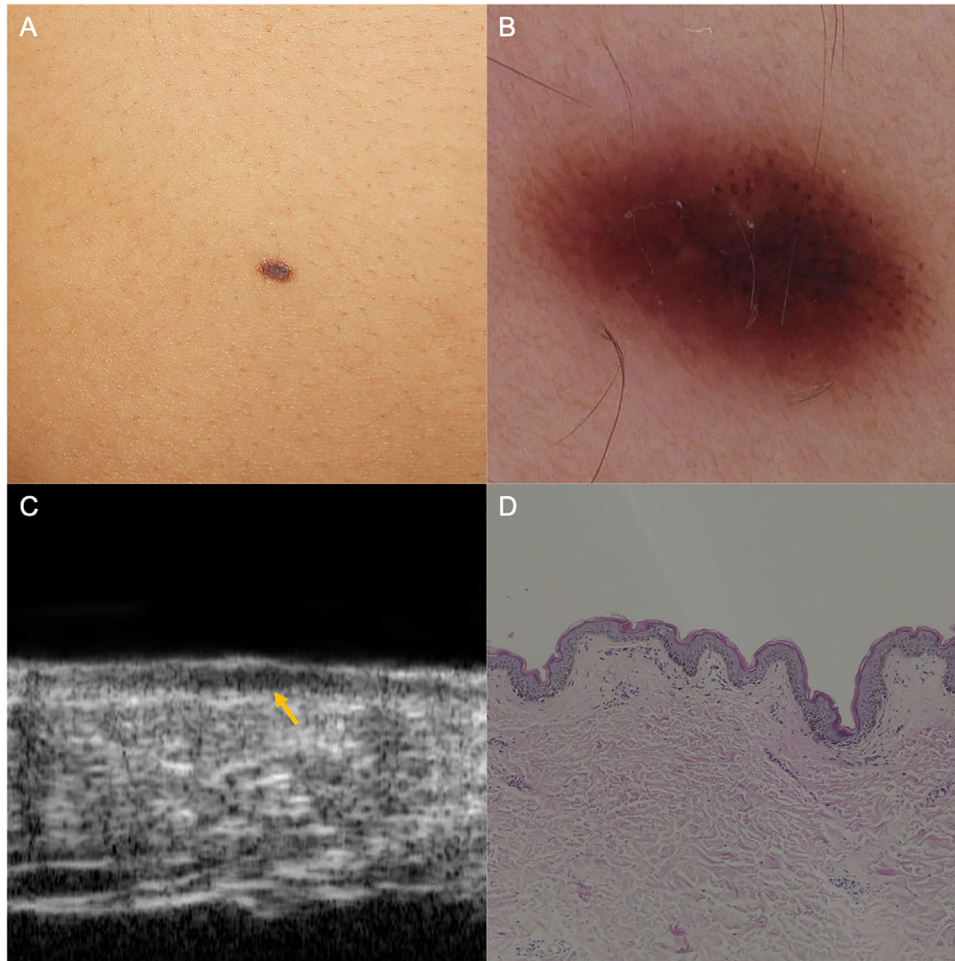


FIGURE 2 Junctional nevus. (A) A well-defined brown macule on the abdomen. (B) Dermoscopic examination revealed regular reticular and globular pattern. (C) HF-US at 50 MHz showed a strip-shaped hypoechoic area beneath the epidermis (yellow arrow). (D) Histopathology confirmed the nevus cell nests restricted in the dermal-epidermal junction (hematoxylin-eosin, original magnification $\times 50$). HF-US, high-frequency ultrasound

The thin nature of the lesions on HF-US might be related to the extremely restricted nevus cell nests in the dermal-epidermal junction. We might improve the ability to detect the junctional nevi if we could apply the ultrasound probe with even higher frequency in the future. While in compound nevi and intradermal nevi, we first proposed two new HF-US features, namely straw-hat sign and mushroom sign, to further differentiate MN subtypes. As mentioned above, by comparing with histopathological manifestations, we speculated that the formation of these two ultrasonic features was correlated with the unique arrangement of nevus cell nests and hair follicles in these two subtypes. However, the specificity of them is not 100%, since one compound nevus lesion showed the mushroom sign, and one intradermal nevus lesion showed the straw-hat sign. This could be explained by the difficulty in the histopathological distinguishment of some intradermal nevi and compound nevi lesions. Under these circumstances, referring to clinical and dermoscopic signs might be helpful for further differentiation.

Hyperechoic spots in HF-US have been reported to appear in various cutaneous tumors such as basal cell carcinoma, seborrheic ker-

atosis, trichoepithelioma, and MN,^{10,17} but the mechanisms are still unclear. Previous literature¹⁷ suggested that hyperechoic spots could be associated with calcification, cornified cysts, clusters of parakeratotic or apoptotic cells, or necrosis. In our study, hyperechoic spots were found in 57.6% intradermal nevi (38/66) and not in any other subtypes. We speculated that the hyperechoic spots inside the MN might correlate to the melanin accumulation. However, the correlation needs further histopathological confirmation.

Our study has several limitations. First, this was a retrospective study, so inevitable inherent biases and variations existed. Second, because HF-US evaluation was not a regular procedure for MN lesions, the sample size of this study is relatively small. Third, since MN lesions are benign, we used clinical and dermoscopic criteria for MN diagnosis as well as subtype classification, and the correlations between ultrasonic features and pathological changes were not fully investigated in all the lesions. At last, we did not include other cutaneous tumors for comparison, so this study remains a preliminary descriptive study complementing previous researched on the ultrasonic features of MN more comprehensively.

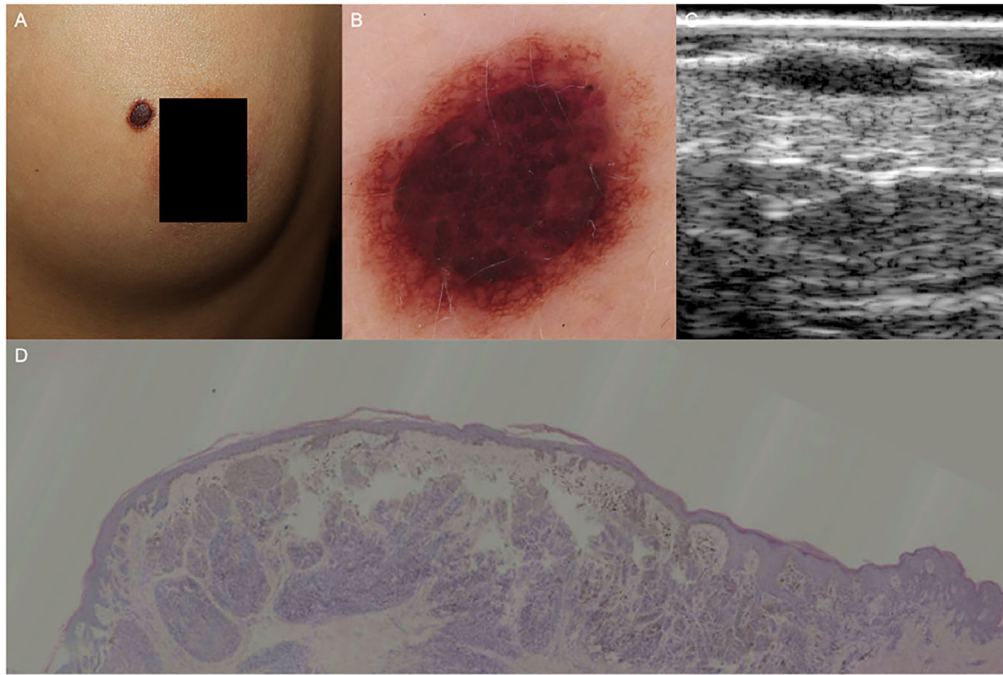
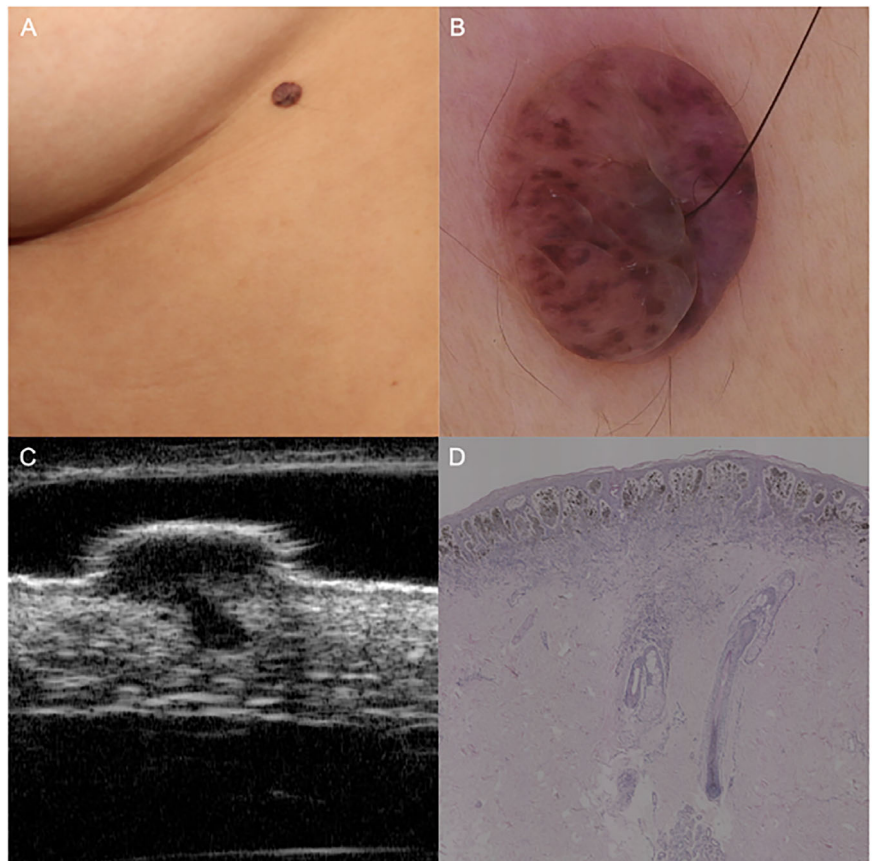


FIGURE 3 Compound nevus. (A) An elevated dark-brown papule on the left breast. (B) Dermoscopic examination revealed central cobblestone and peripheral reticular pattern. (C) HF-US at 20 MHz showed a typical straw-hat sign. (D) Histopathology confirmed the dermal nevus cell aggregation at the lesion center (the cap under HF-US), and the continuous band-like nevus cell nests in the dermal-epidermal junction at the lesion periphery (the brim under HF-US), (hematoxylin-eosin, original magnification $\times 25$). HF-US, high-frequency ultrasound

FIGURE 4 Intradermal nevus. (A) A soft and brown nodule on the left lateral chest, with a terminal hair penetrating through the center. (B) Dermoscopic examination revealed globular pattern with a terminal hair. (C) HF-US at 50 MHz showed a typical mushroom sign. (D) Histopathologic investigation demonstrated a vast number of dermal nevus cells in the papillary dermis (the umbrella under HF-US) and the ensheathing of a hair follicle (the stalk under HF-US) (hematoxylin-eosin, original magnification $\times 25$). HF-US, high-frequency ultrasound



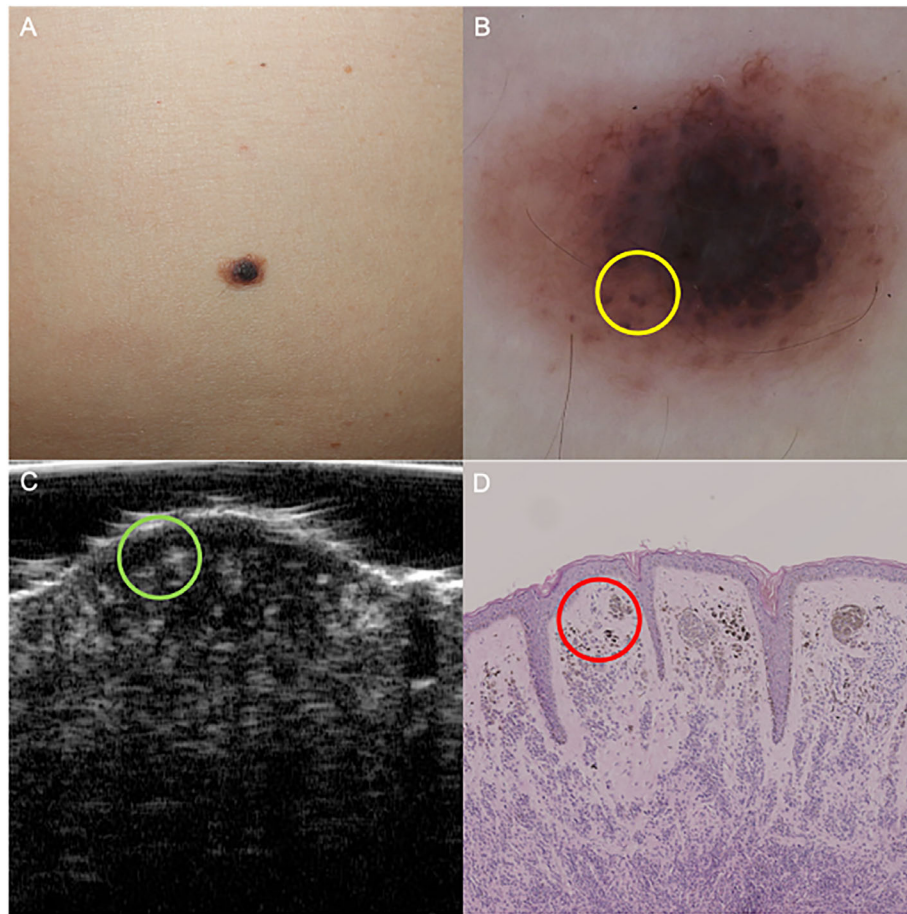


FIGURE 5 An intradermal nevus lesion revealing hyperechoic spots under HF-US examination. (A) An elevated, brown-to-dark papule on the abdomen. (B) Dermoscopy showed globular pattern (yellow circle) and scattered pigment networks. (C) HF-US at 50 MHz demonstrated a well-defined hypoechoic structure in the upper dermis with multiple hyperechoic spots (green circle). (D) Histopathology confirmed the pigment aggregation in the reticular dermis (red circle). HF-US, high-frequency ultrasound

5 | CONCLUSION

Our study firstly reported the detailed HF-US features of MN according to its subtypes. HF-US showed a satisfying consistency with clinical and dermoscopic classification of MN subtypes and is expected to provide more objective information revealing internal morphological features for subtype classification and differential diagnosis of MN lesions.

ACKNOWLEDGMENTS

This work is supported by The Non-profit Central Research Institute Fund of Chinese Academy of Medical Sciences (grant number: 2019XK320024), the National Natural Science Foundation of China (grant number: 61871011) and the CAMS Innovation Fund for Medical Sciences (CIFMS) (grant number: 2020-I2M-C&T-B-033).

FUNDING INFORMATION

The Non-profit Central Research Institute Fund of Chinese Academy of Medical Sciences, Grant Number: 2019XK320024; The National Natural Science Foundation of China, Grant Number: 61871011; The CAMS Innovation Fund for Medical Sciences (CIFMS): 2020-I2M-C&T-B-033.

CONFLICT OF INTEREST

The authors declare that there is no conflict of interest that could be perceived as prejudicing the impartiality of the research reported.

ORCID

Yu-Kun Wang  <https://orcid.org/0000-0001-6304-9379>

Qing-Li Zhu  <https://orcid.org/0000-0002-0618-2381>

Jun-cheng Wang  <https://orcid.org/0000-0003-0972-9511>

REFERENCES

- Whiteman DC, Pavan WJ, Bastian BC. The melanomas: a synthesis of epidemiological, clinical, histopathological, genetic, and biological aspects, supporting distinct subtypes, causal pathways, and cells of origin. *Pigment Cell Melanoma Res.* 2011;24(5):879–97.
- Damsky WE, Bosenberg M. Melanocytic nevi and melanoma: unraveling a complex relationship. *Oncogene* 2017;36(42):5771–92.
- Whiteman DC, Brown RM, Purdie DM, Hughes MC. Melanocytic nevi in very young children: the role of phenotype, sun exposure, and sun protection. *J Am Acad Dermatol.* 2005;52(1):40–7.

4. De Giorgi V, Gori A, Greco A, Savarese I, Alfaioli B, Grazzini M, et al. Sun-protection behavior, pubertal development and menarche: factors influencing the melanocytic nevi development-the results of an observational study of 1,512 children. *J Invest Dermatol*. 2018;138(10):2144–51.
5. Carrera C, Marchetti MA, Dusza SW, Argenziano G, Braun RP, Halpern AC, et al. Validity and reliability of dermoscopic criteria used to differentiate nevi from melanoma: a web-based international dermoscopy society study. *JAMA Dermatol*. 2016;152(7):798–806.
6. Tognetti L, Cevenini G, Moscarella E, Cinotti E, Farnetani F, Mahlvey J, et al. An integrated clinical-dermoscopic risk scoring system for the differentiation between early melanoma and atypical nevi: the iDScore. *J Eur Acad Dermatol Venereol*. 2018;32(12):2162–70.
7. Woltsche N, Schmid-Zalaudek K, Deinlein T, Rammel K, Hofmann-Wellenhof R, Zalaudek I. Abundance of the benign melanocytic universe: dermoscopic-histopathological correlation in nevi. *J Dermatol*. 2017;44(5):499–506.
8. Almuhanha N, Wortsman X, Wohlmuth-Wieser I, Kinoshita-Ise M, Alhusayen R. Overview of ultrasound imaging applications in dermatology. *J Cutan Med Surg*. 2021;25(5):521–9.
9. Bhatt KD, Tambe SA, Jerajani HR, Dhurat RS. Utility of high-frequency ultrasonography in the diagnosis of benign and malignant skin tumors. *Indian J Dermatol Venereol Leprol*. 2017;83(2):162–82.
10. Qin J, Wang J, Zhu Q, Liu J, Gao Y, Wang Y, et al. Usefulness of high-frequency ultrasound in differentiating basal cell carcinoma from common benign pigmented skin tumors. *Skin Res Technol*. 2021;27(5):766–73.
11. Argenziano G, Soyer HP, Chimenti S, Talamini R, Corona R, Sera F, et al. Dermoscopy of pigmented skin lesions: results of a consensus meeting via the internet. *J Am Acad Dermatol*. 2003;48(5):679–93.
12. Grajdeanu IA, Vata D, Statescu L, Popescu IA, Porumb-Andrese E, Patrascu AI, et al. Use of imaging techniques for melanocytic naevi and basal cell carcinoma in integrative analysis (review). *Exp Ther Med*. 2020;20(1):78–86.
13. Li QX, Swanson DL, Tu P, Yang SX, Li H. Clinical and dermoscopic features of surgically treated melanocytic nevi: a retrospective study of 1046 cases. *Chin Med J (Engl)*. 2019;132(17):2027–32.
14. Harland CC, Kale SG, Jackson P, Mortimer PS, Bamber JC. Differentiation of common benign pigmented skin lesions from melanoma by high-resolution ultrasound. *Br J Dermatol*. 2000;143(2):281–9.
15. Hauschild A, Egberts F, Garbe C, Bauer J, Grabbe S, Hamm H, et al. Melanocytic nevi. *J Dtsch Dermatol Ges*. 2011;9(9):723–34.
16. Sardana K, Chakravarty P, Goel K. Optimal management of common acquired melanocytic nevi (moles): current perspectives. *Clin Cosmet Investig Dermatol*. 2014;7:89–103.
17. Uhara H, Hayashi K, Koga H, Saida T. Multiple hypersonographic spots in basal cell carcinoma. *Dermatol Surg*. 2007;33(10):1215–9.

How to cite this article: Wang Y-K, Gao Y-J, Liu J, Zhu Q-L, Wang J-c, Qin J, et al. A comparative study of melanocytic nevi classification with dermoscopy and high-frequency ultrasound. *Skin Res Technol*. 2022;28:265–273.
<https://doi.org/10.1111/srt.13123>